Perpendicular magnetic anisotropy of CoFeB\Ta bilayers on ALD HfO_2

Bart F. Vermeulen, Jackson Wu, Johan Swerts, Sebastien Couet, Iuliana P. Radu, Guido Groeseneken, Christophe Detavernier, Johanna K. Jochum, Margriet Van Bael, Kristiaan Temst, Amit Shukla, Shinji Miwa, Yoshishige Suzuki, and Koen Martens

Citation: AIP Advances **7**, 055933 (2017);

View online: https://doi.org/10.1063/1.4978007

View Table of Contents: http://aip.scitation.org/toc/adv/7/5

Published by the American Institute of Physics

Perpendicular magnetic anisotropy of CoFeB\Ta bilayers on ALD HfO_2

Bart F. Vermeulen,[1,a] Jackson Wu,[1] Johan Swerts,[1] Sebastien Couet,[1] Iuliana P. Radu,[1] Guido Groeseneken,[1,b] Christophe Detavernier,[2] Johanna K. Jochum,[3] Margriet Van Bael,[3] Kristiaan Temst,[4] Amit Shukla,[5] Shinji Miwa,[5] Yoshishige Suzuki,[5] and Koen Martens[6,c]
[1]*IMEC, Kapeldreef 75, Leuven, Belgium*
[2]*Solid State Physics, Ghent University, 9000 Ghent, Belgium*
[3]*Laboratory of Solid State Physics and Magnetism, KU Leuven, 3001 Leuven, Belgium*
[4]*Instituut voor Kern- en Stralingsfysica, KU Leuven, 3001 Leuven, Belgium*
[5]*Graduate School of Engineering, Osaka University, 565-0871 Osaka, Japan*
[6]*IMEC, Kapeldreef 75, 3001 Leuven, Belgium*

(Presented 3 November 2016; received 22 September 2016; accepted 29 November 2016; published online 6 March 2017)

Perpendicular magnetic anisotropy (PMA) is an essential condition for CoFe thin films used in magnetic random access memories. Until recently, interfacial PMA was mainly known to occur in materials stacks with MgO\CoFe(B) interfaces or using an adjacent crystalline heavy metal film. Here, PMA is reported in a CoFeB\Ta bilayer deposited on amorphous high-κ dielectric (relative permittivity κ=20) HfO_2, grown by atomic layer deposition (ALD). PMA with interfacial anisotropy energy K_i up to 0.49 mJ/m^2 appears after annealing the stacks between 200°C and 350°C, as shown with vibrating sample magnetometry. Transmission electron microscopy shows that the decrease of PMA starting from 350°C coincides with the onset of interdiffusion in the materials. High-κ dielectrics are potential enablers for giant voltage control of magnetic anisotropy (VCMA). The absence of VCMA in these experiments is ascribed to a 0.6 nm thick magnetic dead layer between HfO_2 and CoFeB. The results show PMA can be easily obtained on ALD high-κ dielectrics. [http://dx.doi.org/10.1063/1.4978007]

Perpendicular magnetic anisotropy materials are key enablers for spintronics and high retention magnetic random access memory technologies. Thin films composed of Co, Fe and B have been thoroughly investigated and, adjacent to suitable materials, display PMA when they are sufficiently thin.[1,2] The PMA of Co(Fe)(B) is often ascribed to interfacial anisotropy, with reported values for the interfacial anisotropy energy K_i in the order of 1.5 mJ/m^2/interface.[1,2] Two types of interfaces are inducing PMA in ferromagnetic (FM) thin films: the interface with a crystalline heavy metal, and the interface with an oxide. A crystalline heavy metal can induce PMA through spin orbit coupling,[3] and the PMA depends critically on the sharpness of the interface.[4,5]

The origin of PMA at the interface between a ferromagnet and an oxide lies in the hybridization of the FM $3d_z$ orbitals and the oxide $2p_{xy}$ and $2p_{yz}$ orbitals (corresponding to Fe-O and Co-O bonds).[6,7] The PMA is mainly known to occur at the interface with MgO.[1,2,8] Additionally, ferromagnetic thin films deposited on amorphous oxides like thermally grown SiO_2 can also show PMA.[9]

This paper presents a study of the PMA of a CoFeB\Ta bilayer deposited on an amorphous high-κ dielectric, atomic layer deposition grown HfO_2. Previous PMA reports on high-κ dielectrics

[a]Electronic mail: bart.vermeulen@imec.be; Instituut voor Kern- en Stralingsfysica, KU Leuven, 3001, Leuven, Belgium.
[b]Department of Electrical Engineering, KU Leuven, 3001, Leuven, Belgium.
[c]Laboratory for Semiconductor Physics, KU Leuven, 3001, Leuven, Belgium.

use either a thermally grown dielectric[10] or introduce an interface known to induce PMA, such as the Co\Pt interface.[11] ALD growth allows to deposit high-κ oxides with a high dielectric breakdown quality[12] and keeping the oxide amorphous solves possible lattice mismatch issues. The higher κ value of HfO_2 allows to enhance the amount of accumulated interfacial charges upon the application of an electric field. This opens the door for novel applications using interesting effects such as VCMA, that has already been largely reported using MgO.[10,13,14] This is the first report of PMA in CoFeB\Ta bilayers on amorphous ALD high-κ dielectrics, and is of potential interest for low power MRAM applications and spintronics.

Samples are fabricated on a Si wafer after an O_3 based clean leaving 1 nm of chemical SiO_2. A forming gas anneal at 420°C for 20 minutes is applied to passivate dangling bonds, after which 2.5 nm of amorphous[15] wet ALD HfO_2 is deposited at 300°C in an ASM Polygon 8300 reactor. The samples are transferred to a Canon Anelva PVD reactor, the HfO_2 layer is degassed in UHV at 350°C for 5 min, and a CoFeB wedge with thickness ranging from 0.6 to 2.4 nm is sputter-deposited. Finally, 2 nm of Ta followed by 5 nm of Ru are sputter-deposited. Samples are annealed at temperatures between 100 and 350°C at atmospheric pressure for 10 min in N_2 ambient.

In-situ X-ray diffraction (XRD) is performed in a Bruker D8 Discover equipped with a home-built annealing chamber at a constant heating rate of 0.5°C/sec. The XRD pattern is recorded in a fixed 20° 2θ window. TEM and energy dispersive X-ray spectroscopy (EDS) specimens are prepared using conventional ion milling and observed in a FEI Titan at 300kV. Rutherford backscattering spectra (RBS) were obtained using a He^+ beam with an energy of 1.523 MeV, at a scattering angle of 170° and sample tilt angle of 11°.

Room temperature superconducting quantum interference device (SQUID) magnetization measurements have been performed in a LOT-Quantum Design MPMS XL-5. Vibrating sample magnetometry (VSM) measurements were performed using a Microsense EV11 tool.

In-Situ X-Ray Diffraction (XRD) is used to probe the crystalline quality of the multilayer stack. The XRD-curves were recorded at increasing temperatures and can be found in the inset of Fig. 1 for selected temperatures. The main feature visible in the spectrum is the peak at a 2θ value of 41.9° (see inset). This peak is attributed to the hcp Ru (002) plane, although it slightly differs from the value (42.176°) reported by Wyckoff et al.[16] This offset is related to a small misalignment of the sample stage. The fringes visible in the inset of Fig. 1 are indicative of the planar nature of the Ru layer. The increasing intensity of these peaks with temperature indicates the increasing crystalline quality of the Ru thin film. No peak characteristic of CoFe can be detected (the expected (002) peak at 65.8° is absent, not shown), likely due to its low intensity. Finally, no HfO_2 peak can be detected. The HfO_2 is likely amorphous as deposited[15] and the monoclinic (11-1) peak at 28.2°[17] appears after the in situ measurement (i.e. annealing at 1000°C: not shown, outside of the in situ 2θ window). The high-temperature stability of the films can also be assessed with in-situ XRD, as shown in Fig. 1. The

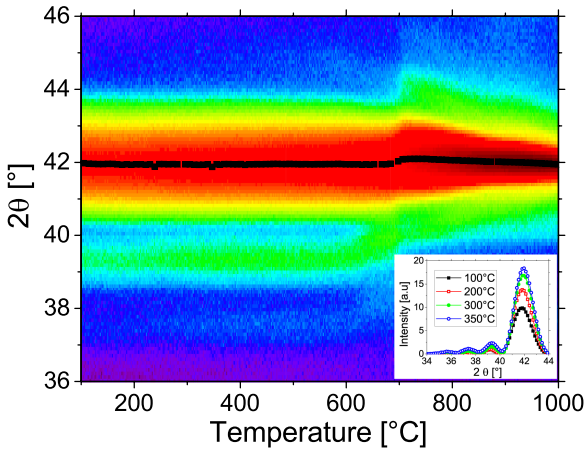

FIG. 1. Two dimensional plot of the XRD $\theta - 2\theta$ amplitude in function of the sample temperature. The black dots indicate the position of the central peak. The inset shows individual curves at the given temperatures.

characteristic is stable as a function of temperature up to $T_a = 700°C$, where the Ru fringes disappear and the Ru peak shifts upwards.

Room temperature transmission electron microscopy images for as-deposited and annealed stacks are shown in Figure 2. Unlike a Co\Pt bilayer deposited onto ALD HfO_2,[11] CoFeB\Ta bilayers do not undergo visible epitaxial reordering of the interface after anneal. This is ascribed to the particularly small CoFeB grain size, making it look like the layer is amorphous in TEM (the cross-sectional TEM signal is integrated over the thickness of the sample; when grains with different in-plane orientation and a size in the order of the thickness of the thin film -1 nm-constitute the layer, different grains cannot be distinguished). The thickness of the layers does not change upon annealing at 300°C, however, a significant thickness increase in CoFeB (+55%) and Ta (+121%) is seen after annealing at 350°C. Such a large volume increase has not been reported in MgO\CoFeB\Ta stacks or in HfO_2\Co\Pt stacks.[11] Additional experiments may be necessary to investigate the origin of this volume increase.

To investigate the possible origin of this thickness increase, energy-dispersive X-ray spectroscopy (EDS) measurements are used, to probe depth resolved atomic concentrations. In Figure 3, three EDS profiles for an as-deposited (AD) and an annealed (300 and 350°C) sample are shown. The layers in the as-deposited stack of Figure 3 a) and the stack annealed at 300°C b) show little interdiffusion. After annealing at 350°C for 10 minutes (see Figure 3 c)), tantalum, cobalt, iron and likely boron have diffused all the way between the HfO_2 and the Ru layer. The resulting layer between HfO_2 and Ru is an amorphous CoFeBTaO alloy. Boron outdiffusion upon annealing a CoFeB thin film is expected,[18,19] and likely leads to crystalline reordering of CoFe as well as a thickness increase in the Ta layer[19] adjacent to the CoFeB. Diffusion of Ta into the CoFeB has been reported as well,[20] and broadens the CoFeB\Ta interface, likely deteriorating the PMA. Significant oxygen content is also visible throughout the CoFeBTa layer, and likely originates from both the HfO_2 layer and the annealing ambient. The absorption of O in the CoFeBTa layer may account for a significant increase in the thickness. The absorbed O can originate from either the HfO_2 layer or the environment. However, given the amount of oxygen in CoFeBTa and HfO_2, it is likely that a large fraction of O is adsorbed from the atmosphere. The Ru layer has not visibly interdiffused.

In summary, the structural analysis with XRD, EDS and TEM has shown that O, Co, Fe, Ta and likely B completely interdiffuse between the HfO_2 and Ru layers upon annealing at 350°C. No epitaxial reordering of the interface between CoFeB and Ta is seen after anneal. TEM additionally shows an increase in the thickness of the original CoFeB layer, which is likely due to the strong interdiffusion and O absorption caused by the annealing treatment.

Polar magneto-optical Kerr effect (pMOKE) measurements probe the perpendicular component of the magnetization. They provide insight in the evolution of the magnetic anisotropy as a function of the annealing temperature and the CoFeB thickness, and allow to select two annealing temperatures for further investigation with VSM. The CoFeB thickness data is interpolated from points measured with Rutherford backscattering spectroscopy (RBS) along the CoFeB thickness wedge (RBS data not

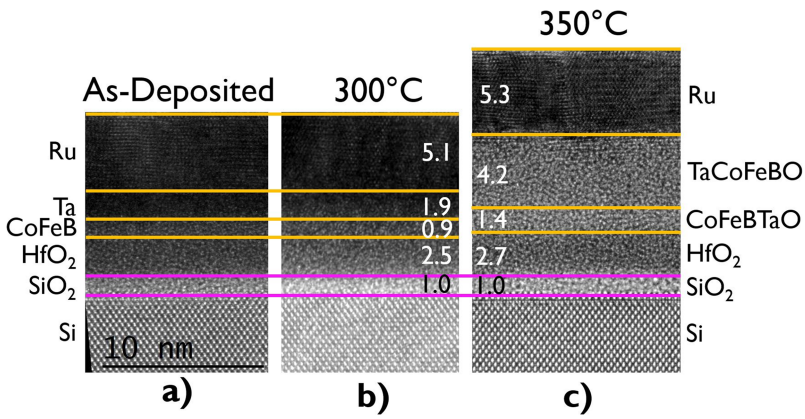

FIG. 2. Room temperature TEM images of the materials stacks. a) Micrograph of an as-deposited stack. b) Micrograph of a stack annealed at 300°C and c) 350°C for 10 min in N_2.

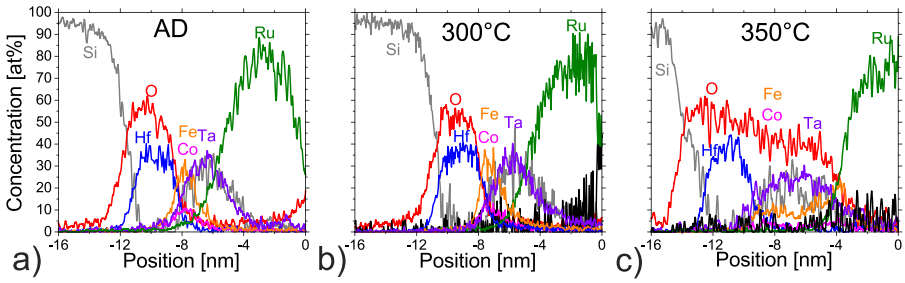

FIG. 3. Energy-Dispersive X-Ray Spectroscopy (EDS) mapping of the surface layers. The curves display the atomic concentration profiles for Si, O, Hf, Co, Fe, Ta and Ru. In both figures, there is an increase in the Si signal intensity at the location of the Ta layer, due to the partial overlap of the Si K peak and the Ta M peak. a) Profiles measured on an as-deposited stack. b) Profiles for a stack annealed at 300°C and c) 350°C for 10 min in N_2.

shown). As can be seen in Figure 4, the as-deposited samples do not show PMA. The PMA appears only after annealing at temperatures between 200°C and 350°C depending on the thickness of the CoFeB layer. As the annealing temperature increases even further, the interdiffusion of Ta and O into the CoFeB film (Fig. 3) coincides with the almost complete loss of PMA. Hence, T_a = 200 °C and 300 °C are chosen for further investigation.

The thickness dependence of the magnetic moment after annealing at 200°C and 300°C is shown in Fig. 5 a). The volume magnetization M_s of CoFeB is calculated from the slope of the volume magnetic moment taking into account the fixed area for all samples. M_s increases strongly with the temperature of the annealing treatment, from 1.41x10^{6}A/m at 200°C to 2.34x10^{6}A/m at 300°C. Interpolating the thickness dependence of M_s towards zero magnetic moment allows to detect the presence of a magnetic dead layer (MDL). The thickness of the MDL increases from 0.19 nm at 200°C to 0.63 nm at 300°C. Both the increase in magnetization and in dead layer thickness can be ascribed to the annealing treatment. As B diffuses out of CoFeB, the crystallinity of the resulting CoFe is thought to improve[18,19] and the magnetic moment increases.[21] Ta is known to induce a MDL at the interface with CoFeB,[10,22] depending on the morphology and the annealing conditions. The

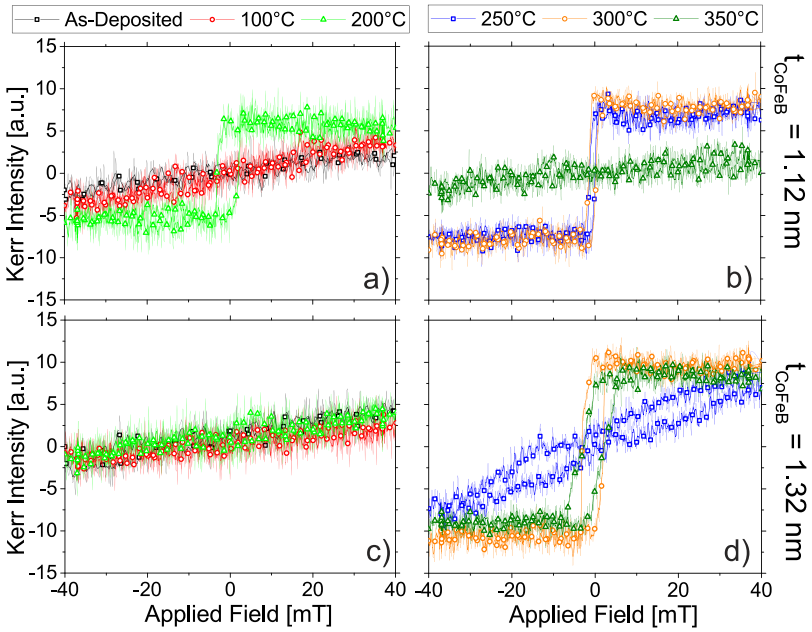

FIG. 4. MOKE data for a CoFeB thickness of 1.12 nm and 1.32 nm before and after annealing for 10 min in N_2 at a given temperature.

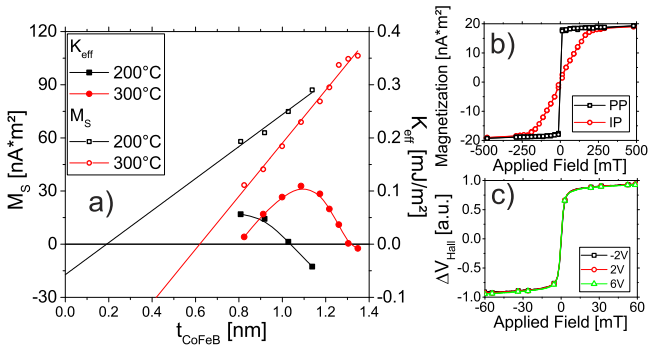

FIG. 5. a) Net magnetic moment M_s and effective anisotropy energy K_{eff} for 8x8 mm^2 samples annealed at 200°C and 300°C as a function of the measured CoFeB thickness. The straight lines indicate the linear fit to the M_s data, and the extrapolation to zero magnetic moment gives the thickness of the magnetic dead layer. b) SQUID measurement for samples with a t_{CoFeB} = 0.91 nm and an area of 25 mm^2. c) Anomalous Hall effect measurement on a sample annealed at 300°C with a CoFeB thickness of 1.32 nm.

oxygen diffusing out of the HfO_2 into the CoFeB also likely induces a MDL at the HfO_2/CoFeB interface. The MDL thickness seen in Fig. 5 a) contains a contribution from both the HfO_2/CoFeB and CoFeB/Ta interfaces.

The effective anisotropy energy K_{eff} can be evaluated by measuring the area between the hard axis and easy axis magnetization curves for a given sample. The K_{eff} as a function of the CoFeB thickness for samples annealed at 200°C and 300°C is shown in Fig. 5 a). The increase of the MDL thickness with annealing temperature is reflected in a slightly smaller increase in the critical thickness t_c of the CoFeB from 1.02 nm to 1.3 nm, defined as the thickness where the magnetic anisotropy of the thin film changes from PMA to in plane. The interfacial anisotropy K_i is determined by extrapolating the linear part of K_{eff} towards the MDL thickness, essentially extrapolating the K_{eff} to zero magnetic thickness. Alternatively, Equation 1 can be used:

$$K_i = K_{eff} - \left(K_v + \frac{\mu_0 M_s^2}{2}\right)(t_{Co} - t_{DL}) \tag{1}$$

where K_v is the geometrical bulk anisotropy of the CoFeB thin film, calculated as dK_{eff}/dt_{CoFeB} in the linear region of the curve. The measured values for M_s, K_i, K_v and t_{MDL} are summarized in Table I.

Hall measurements are used to probe the presence of VCMA at the interface between HfO_2 and CoFeB and are shown in Figure 5 c). The curves collected at different applied gate voltages overlap perfectly, showing no VCMA could be detected, despite the high electric fields applied across the HfO_2. In HfO_2\Co\Pt[11] the absence of VCMA was ascribed to any combination of the following three factors: a MDL at the HfO_2\Co interface, Co itself which shows only small VCMA and the remote Co\Pt interface which induces PMA. Here, the absence of VCMA is ascribed to the significant magnetic dead layer present at the interface, and at higher annealing temperatures the degraded magnetic properties of the stacks due to the significant interdiffusion of oxygen and tantalum.

In conclusion, the magnetic anisotropy of HfO_2\CoFeB\Ta trilayers has been investigated as a function of the annealing temperature and CoFeB thickness. PMA appears after annealing at temperatures between 200°C and 350°C. TEM and EDS characterization has shown that strong interdiffusion happens at 350°C, which correlates with the suppression of PMA. No VCMA is observed at the interface between HfO_2 and CoFeB. This is ascribed to the thick magnetic dead layer at the HfO_2\CoFeB

TABLE I. Magnetic anisotropy energies for HfO_2\CoFeB\Ta in function of the annealing temperature

T_a [°C]	M_s [MA/m]	K_i [mJ/m^2]	K_v [MJ/m^3]	t_{MDL} [nm]
200	1.41	0.344	-1.65	0.2
300	2.34	0.49	-4.16	0.63

interface. The reported results show that PMA can be obtained at the interface between a ferromagnetic thin film and an amorphous ALD high-κ dielectric.

ACKNOWLEDGMENTS

We wish to acknowledge Johan Meersschaut for fruitful discussions on RBS, Hugo Bender for assisting in the analysis of TEM micrographs and EDS spectra, as well as Sofie Mertens, Yoann Tomczak, Aaron Thean, Andre Stesmans and Valeri Afanasiev. We acknowledge the financial support of FWO Flanders through grant N° ZKD0303-00-W01.

[1] S. Ikeda, K. Miura, H. Yamamoto, K. Mizunuma, H. Gan, M. Endo, S. Kanai, J. Hayakawa, F. Matsukura, and H. Ohno, "A perpendicular-anisotropy CoFeB–MgO magnetic tunnel junction," Nature Materials **9**, 721–724 (2010).
[2] T. Liu, J. Cai, and L. Sun, "Large enhanced perpendicular magnetic anisotropy in CoFeB/MgO system with the typical Ta buffer replaced by an Hf layer," AIP Advances **2**, 032151 (2012).
[3] P. Bruno, "Tight-binding approach to the orbital magnetic moment and magnetocrystalline anisotropy of transition-metal monolayers," Physical Review B **39**, 865 (1989).
[4] T. Devolder, "Light ion irradiation of Co/Pt systems: structural origin of the decrease in magnetic anisotropy," Physical Review B **62**, 5794 (2000).
[5] S. Bandiera, R. Sousa, B. Rodmacq, and B. Dieny, "Enhancement of perpendicular magnetic anisotropy through reduction of Co-Pt interdiffusion in (Co/Pt) multilayers," Applied Physics Letters **100**, 142410 (2012).
[6] H. Yang, M. Chshiev, B. Dieny, J. Lee, A. Manchon, and K. Shin, "First-principles investigation of the very large perpendicular magnetic anisotropy at Fe—MgO and Co—MgO interfaces," Physical Review B **84**, 054401 (2011).
[7] B. Rodmacq, S. Auffret, B. Dieny, S. Monso, and P. Boyer, "Crossovers from in-plane to perpendicular anisotropy in magnetic tunnel junctions as a function of the barrier degree of oxidation," Journal of Applied Physics **93**, 7513–7515 (2003).
[8] S. Yakata, H. Kubota, Y. Suzuki, K. Yakushiji, A. Fukushima, S. Yuasa, and K. Ando, "Influence of perpendicular magnetic anisotropy on spin-transfer switching current in CoFeB/MgO/CoFeB magnetic tunnel junctions," Journal of Applied Physics **105**, 07D131 (2009).
[9] L. Nistor, B. Rodmacq, S. Auffret, and B. Dieny, "Pt/Co/oxide and oxide/Co/Pt electrodes for perpendicular magnetic tunnel junctions," Applied Physics Letters **94**, 012512 (2009).
[10] K. Kita, D. W. Abraham, M. J. Gajek, and D. Worledge, "Electric-field-control of magnetic anisotropy of Co(0.6)Fe(0.2)B(0.2)/oxide stacks using reduced voltage," Journal of Applied Physics **112**, 033919 (2012).
[11] B. F. Vermeulen, J. Wu, J. Swerts, S. Couet, D. Linten, I. P. Radu, K. Temst, G. Rampelberg, C. Detavernier, G. Groeseneken, and K. Martens, "Perpendicular magnetic anisotropy of Co\Pt bilayers on ALD HfO_2," Journal of Applied Physics **120**, 163903 (2016).
[12] M. Kassmi, F. Jomni, P. Gonon, O. Khaldi, L. Latu-Romain, C. Mannequin, A. Bsiesy, S. Basrour, and B. Yangui, "Reliability of HfO_2 metal–insulator–metal capacitors under AC stress," Journal of Physics D: Applied Physics **49**, 165502 (2016).
[13] T. Maruyama, Y. Shiota, T. Nozaki, K. Ohta, N. Toda, M. Mizuguchi, A. Tulapurkar, T. Shinjo, M. Shiraishi, S. Mizukami, *et al.*, "Large voltage-induced magnetic anisotropy change in a few atomic layers of iron," Nature Nanotechnology **4**, 158–161 (2009).
[14] T. Nozaki, A. Kozioł-Rachwał, W. Skowroński, V. Zayets, Y. Shiota, S. Tamaru, H. Kubota, A. Fukushima, S. Yuasa, and Y. Suzuki, "Large voltage-induced changes in the perpendicular magnetic anisotropy of an MgO-based tunnel junction with an ultrathin Fe layer," Physical Review Applied **5**, 044006 (2016).
[15] A. Delabie, R. L. Puurunen, B. Brijs, M. Caymax, T. Conard, B. Onsia, O. Richard, W. Vandervorst, C. Zhao, M. M. Heyns, *et al.*, "Atomic layer deposition of hafnium oxide on germanium substrates," Journal of Applied Physics **97**, 64104–64104 (2005).
[16] R. Wyckoff, *Crystal Structures 1* (New York, 1963).
[17] S. J. Henderson, O. Shebanova, A. L. Hector, P. F. McMillan, and M. T. Weller, "Structural variations in pyrochlore-structured $Bi_2Hf_2O_7$, $Bi_2Ti_2O_7$ and $Bi_2Hf_{2-x}Ti_xO_7$ solid solutions as a function of composition and temperature by neutron and X-ray diffraction and raman spectroscopy," Chemistry of Materials **19**, 1712–1722 (2007).
[18] H. Kurt, K. Rode, K. Oguz, M. Boese, C. Faulkner, and J. Coey, "Boron diffusion in magnetic tunnel junctions with Mgo (001) barriers and CoFeB electrodes," Applied Physics Letters **96**, 262501 (2010).
[19] S. Karthik, Y. Takahashi, T. Ohkubo, K. Hono, S. Ikeda, and H. Ohno, "Transmission electron microscopy investigation of CoFeB/MgO/CoFeB pseudospin valves annealed at different temperatures," Journal of Applied Physics **106**, 023920 (2009).
[20] C.-W. Cheng, W. Feng, G. Chern, C. Lee, and T.-H. Wu, "Effect of cap layer thickness on the perpendicular magnetic anisotropy in top MgO/CoFeB/Ta structures," Journal of Applied Physics **110**, 033916 (2011).
[21] J. Schmalhorst, A. Thomas, G. Reiss, X. Kou, and A. E., "Influence of chemical and magnetic interface properties of co-fe-b/mgo/co-fe-b tunnel junctions on the annealing temperature dependence of the magnetoresistance," Journal of Applied Physics **102**, 053907–053907 (2007).
[22] K. Oguz, P. Jivrajka, M. Venkatesan, G. Feng, and J. Coey, "Magnetic dead layers in sputtered $Co_{40}Fe_{40}B_{20}$ films," Journal of Applied Physics **103**, 07B526–07B526 (2008).